Supplemental information

Molecular and structural basis of

olfactory sensory neuron axon

coalescence by Kirrel receptors

Jing Wang, Neelima Vaddadi, Joseph S. Pak, Yeonwoo Park, Sabrina Quilez, Christina A. Roman, Emilie Dumontier, Joseph W. Thornton, Jean-François Cloutier, and Engin Özkan
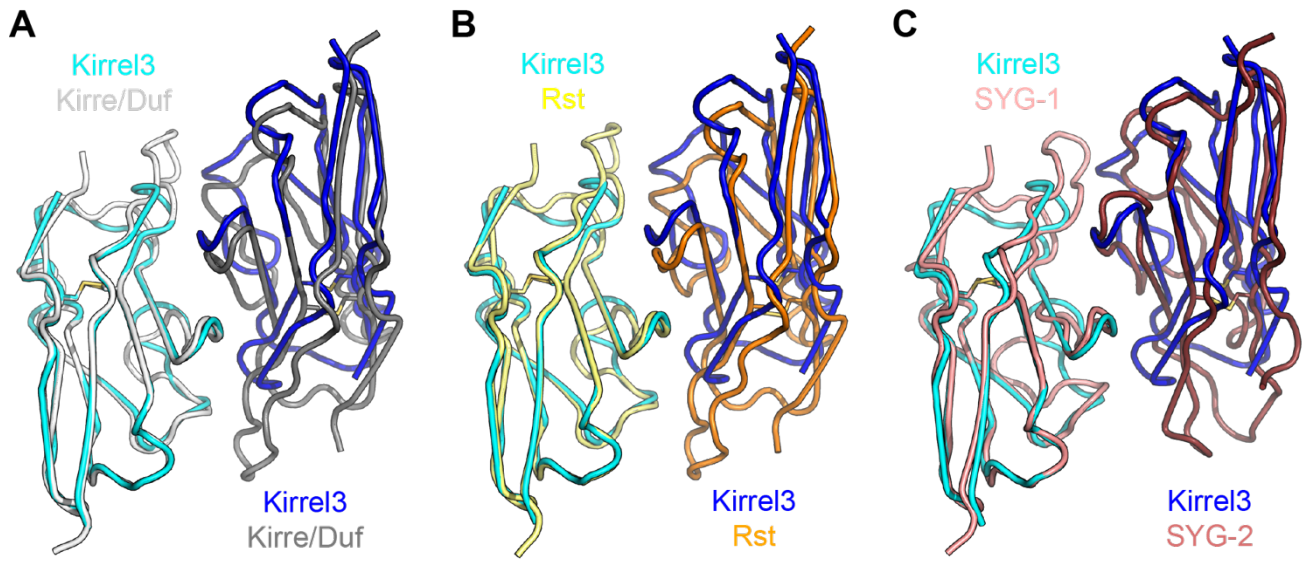
Figure S1. Structural comparison of mouse Kirrel3 D1 with protostome Kirrels, related to Figure 1. Structural comparison of mouse Kirrel3 D1 homodimer with orthologous *Drosophila* Kirre (Duf) D1 homodimer (A), *Drosophila* Rst D1 homodimer (B), and *C. elegans* SYG-1-SYG-2 D1 heterodimer (C). D1 subunits on the left-hand side in all panels have been superimposed to highlight differences in exact dimerization topologies.
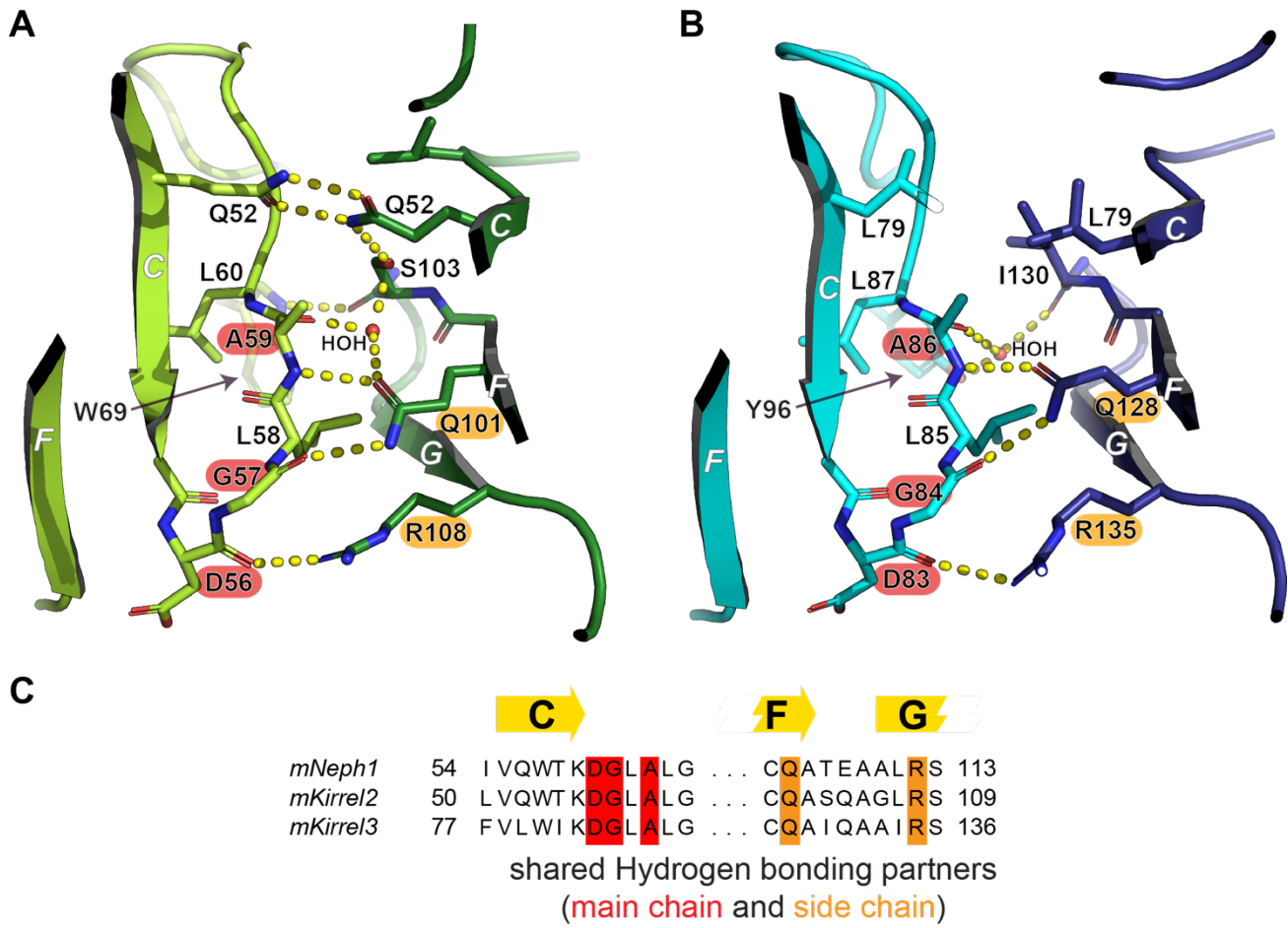
Figure S2. Conserved hydrogen binding networks at the mouse Kirrel homodimerization interfaces, related to Figure 2. Hydrogen bonding networks conserved between Kirrel2 (A) and Kirrel3 (B) homodimerization interfaces. The conserved networks are formed by a Gln and an Arg in F and G strands, respectively (highlighted orange in panels A and B on the structures, and in orange boxes in sequence alignment in panel C), and by main-chain atoms in a conserved stretch in the CD loop (highlighted red).

A

B
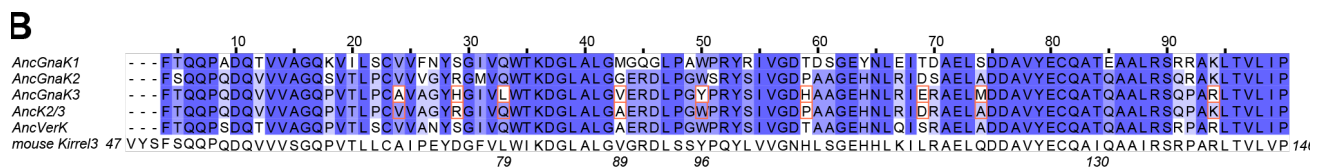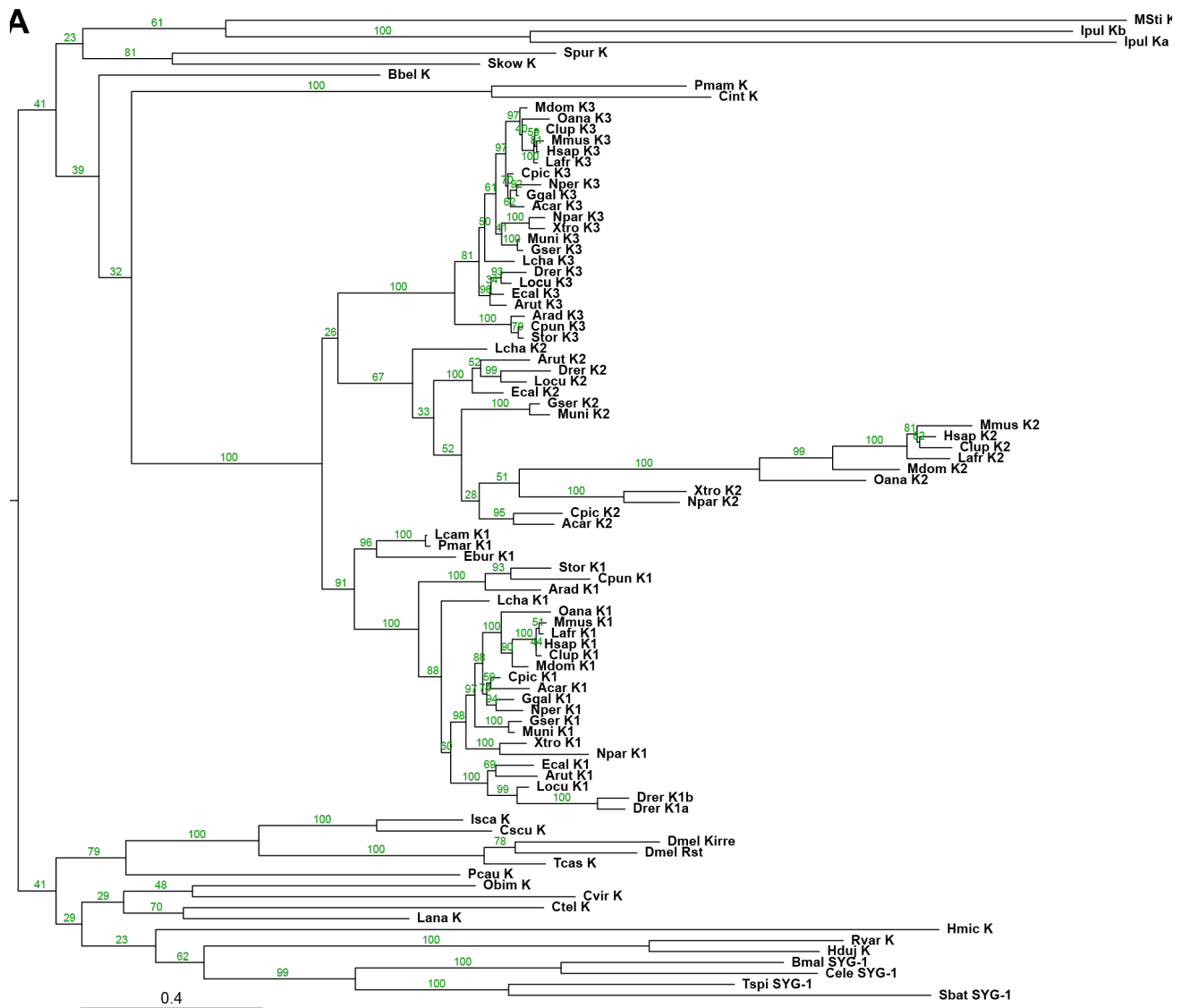
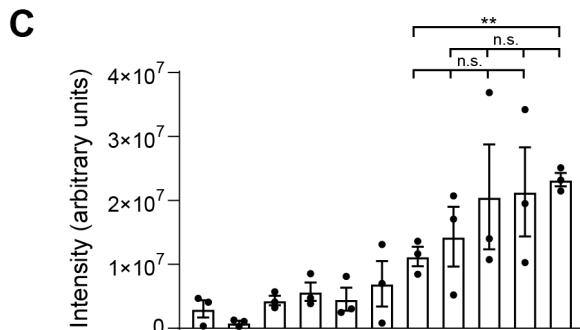□ : positions different between AncK2/3 and AncGnaK3

C

Figure S3.

Figure S3. Phylogenetic analysis of bilaterian Kirrels, related to Figure 3.
(A) Uncollapsed phylogenetic tree for Kirrels with bootstrap support values. Abbreviations for species

3

used: (Mammals) Mmus, *Mus musculus*; Hsap, *Homo sapiens*; Clup, *Canis lupus familiaris*; Lafr, *Loxodonta africana*; Mdom, *Monodelphis domestica*; Oana, *Ornithorhynchus anatinus*; (Aves) Ggal, *Gallus gallus*; Nper, *Nothoprocta perdicaria*; (Reptilia) Acar, *Anolis carolinensis*; Cpic, *Chrysemys picta bellii*; (Amphibia) Xtro, *Xenopus tropicalis*; Npar, *Nanorana parkeri*; Muni, *Microcaecilia unicolor*; Gser, *Geotrypetes seraphini*; (Sarcopterygii) Lcha, *Latimeria chalumnae*; (Actinoptergyii); Ecal, *Erpetoichthys calabaricus*; Arut, *Acipenser ruthenus*; Locu, *Lepisosteus oculatus*; Drer, *Danio rerio*; (Chondrichthyes) Cmil, *Callorhinchus milii*; Arad, *Amblyraja radiata*; Stor, *Scyliorhinus torazame*; Cpun, *Chiloscyllium punctatum*; (Cyclostomata) Pmar, *Petromyzon marinus*; Ebur, *Eptatretus burgeri*; Lcam, *Lethenteron camtschaticum*; (Urochordata) Cint, *Ciona intestinalis*; Pmam, *Phallusia mammillata*; (Cephalochordata) Bbel, *Branchiostoma belcheri*; (Ambulacraria) Spur, *Strongylocentrotus purpuratus*; Skow, *Saccoglossus kowalevskii*; (Xenacoelomorpha) Ipul, *Isodiametra pulchra*; Msti, *Meara stichopi*; (Spiralia) Hmic, *Hymenolepis microstoma*; Ctel, *Capitella teleta*; Lana, *Lingula anatina*; Obim, *Octopus bimaculoides*; Cvir, *Crassostrea virginica*; (Ecdysozoa) Pcau, *Priapulus caudatus*; Dmel, *Drosophila melanogaster*; Tcas, *Tribolium castaneum*; Isca, *Ixodes scapularis*; Cscu, *Centruroides sculpturatus*; Hduj, *Hypsibius dujardini*; Rvar, *Ramazzotius varieornatus*; Cele, *Caenorhabditis elegans*; Bmal, *Brugia malayi*; Tspi, *Trichinella spiralis*; Sbat, *Soboliphyme baturini*. K, K1, K2, and K3 stand for Kirrel, Kirrel1, Kirrel2 and Kirrel3, respectively.

(B) Ancestral vertebrate and gnathostome Kirrel D1 sequences in a multiple sequence alignment with mouse Kirrel3 D1.

(C) Quantitation of intensity values of western blot bands from Figure 3E in the same order. Triplicate data were analyzed using unpaired t-tests. n.s., not significant; **, *p*-value<0.01 (intensity); error bars, ± SEM.
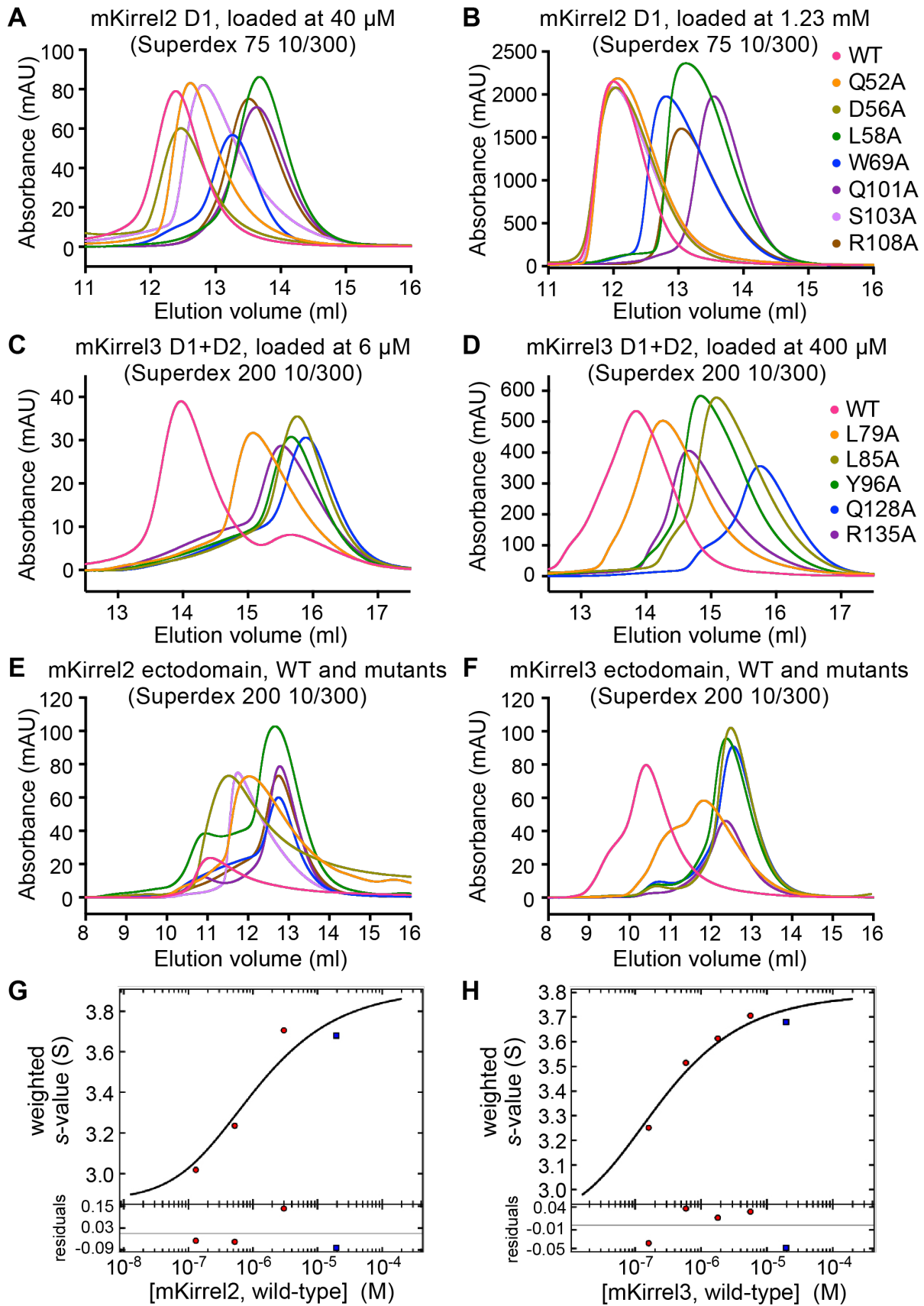
Figure S4. Supplemental biophysical characterization of WT and mutant mouse Kirrel dimerization, related to Figure 4.

(A,B) Size-exclusion chromatography profiles for mouse Kirrel2 D1 mutants loaded at lower (A) and higher concentrations (B).

(C,D) Size-exclusion chromatography profiles for mouse Kirrel3 D1+D2 mutants loaded at lower (C) and higher concentrations (D).

(E,F) Size-exclusion chromatography profiles for mKirrel2 and mKirrel3 WT and mutants loaded at various quantities. The coloring scheme follows that in (B) for mKirrel2 variants (E), and that in (D) for mKirrel3 variants.

(G,H) Binding isotherms for mKirrel2 and mKirrel3 ectodomains plotted as Kirrel concentration against sedimentation coefficients.
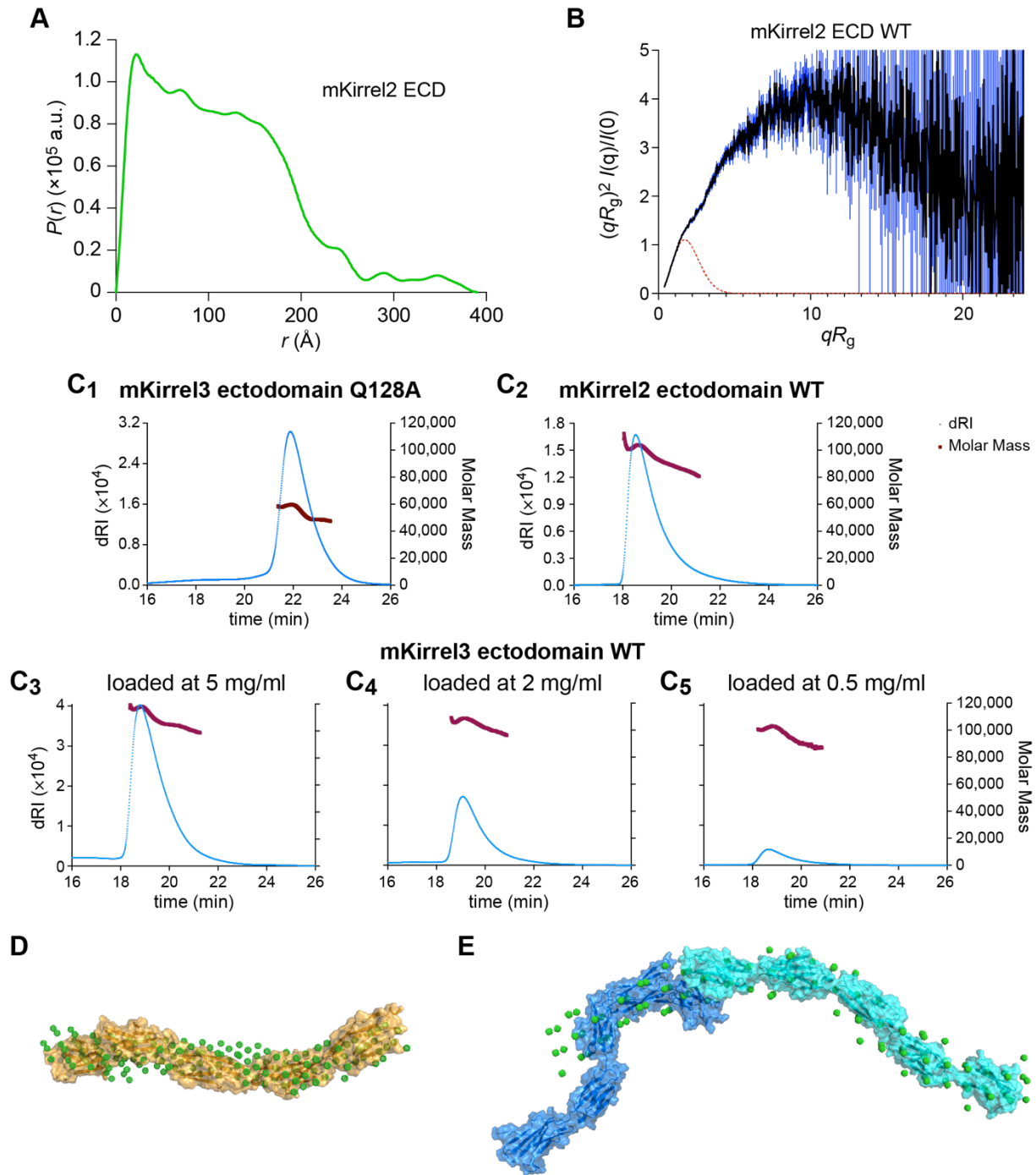
Figure S5. Supplemental SEC-SAXS-MALS analysis of Kirrel ectodomains, related to Figure 5.
(A,B) Pair distance distribution, $P(r)$, (A) and dimensionless Kratky plot for mKirrel2 WT ectodomain (B). Blue vertical lines in (B) are measurement errors. Dashed red lines show predicted plots for a rigid, globular molecule with the same R_g.
(C) Differential refractive index and molar mass measurements for Kirrel ectodomains. See Table S3 for experimental details.
(D) Bead model from *DAMMIF* for mKirrel3 Q128A ectodomain overlayed with the highest prevalence *EOM* model.
(E) Bead model from *DAMMIF* for mKirrel3 WT ectodomain overlayed with the *SASREF* model.

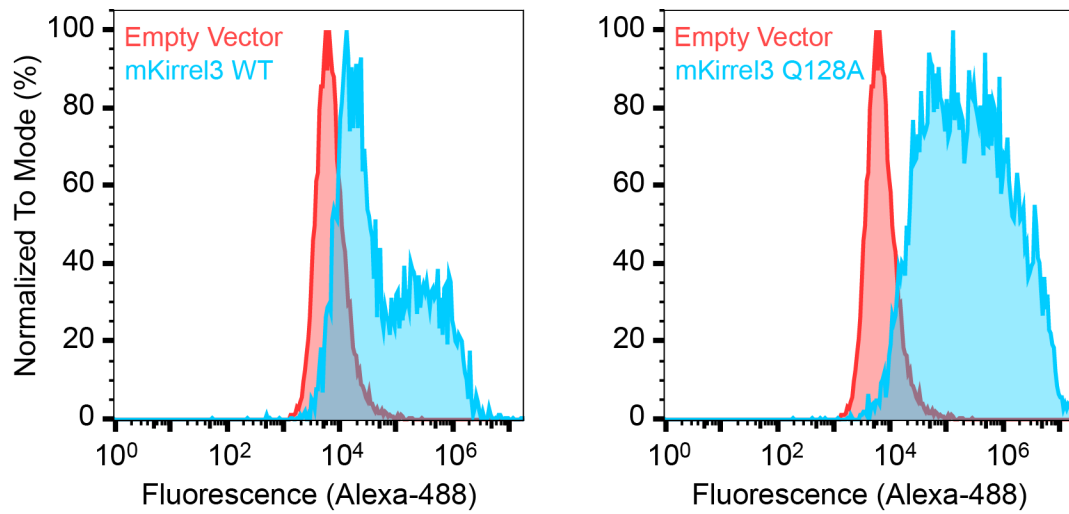**Figure S6. mKirrel3 Q128A is trafficked to cell surface in HEK293 cells, related to Figure 6.** Cell surface display of FLAG-tagged mKirrel3, WT (left) and Q128A mutant (right), on HEK293 cells.

Table S1. Data and refinement statistics for x-ray crystallography, related to Figure 2.

	Mouse Kirrel2 D1	Mouse Kirrel3 D1
Data Collection		
Beamline	SSRL 12-2	APS 24-ID-E
Space Group	*C*2	*P*6$_3$
Cell Dimensions		
a, b, c (Å)	109.14, 48.44, 44.10	63.24, 63.24, 347.81
α, β, γ (°)	90, 107.01, 90	90, 90, 120
Twin law (Fraction)	–	-k,-h,-l (0.31)[†]
Resolution (Å)	50-1.80 (1.83-1.80)*	50-1.95 (1.98-1.95)
R_{sym} (%)	5.6 (17.3)	11.4 (85.3)
$<I>/<\sigma(I)>$	21.9 (5.3)	14.6 (1.9)
$CC_{1/2}$ in the highest resolution bin	0.945	0.617
Completeness (%)	94.2 (69.1)	99.9 (99.8)
Redundancy	3.3 (2.6)	4.4 (4.4)
Refinement		
Resolution (Å)	50-1.80 (1.90-1.80)*	50.1-1.95 (1.98-1.95)
Reflections	19,361	56,984
R_{cryst} (%)	15.49 (19.50)	16.02 (22.95)
R_{free} (%)**	18.09 (25.18)	19.53 (27.48)
Number of atoms		
Protein	1633	6408
Ligand	2	8
Water	337	336
Average B-factors (Å^2)		
All	20.1	38.1
Protein	18.1	38.5
Ligand/Glycans	11.8	44.9
Solvent	30.0	31.4
R.m.s. deviations from ideality		
Bond Lengths (Å)	0.004	0.005
Bond Angles (°)	0.632	0.684
Ramachandran plot		
Favored (%)	98.52	96.19
Outliers (%)	0.00	0.00
Rotamer Outliers (%)	0.00	0.14
All-atom Clashscore[†]	0.00	3.43

* The values in parentheses are for reflections in the highest resolution bin.
** 5% of reflections (971 for Kirrel2 and 2846 for Kirrel3) were not used during refinement for cross validation.
[†] Clashscores and twin fraction were calculated by phenix.refine (*Phenix* version 1.19.1-4122).

Table S2. Data collection details and analysis statistics for SAXS experiments, related to Figure 5.

	mKirrel2 ECD	mKirrel3 ECD	mKirrel3 ECD Q128A
Data Collection and Sample Details			
Experiment setup	SEC-SAXS-MALS		
Instrument	BioCAT facility at APS beamline 18-ID with Pilatus3 X 1M (Dectris) detector		
Wavelength (Å)	1.033		
Camera length (m)	3.655		
q-measurement range (Å^{-1})	0.0044 to 0.35		
Exposure time (s)	0.5		
Exposure period (s)	1.0		
Flow rate (ml/min)	0.6		
Chromatography column	Superdex 200 10/300 Increase		
Buffer	10 mM HEPES pH 7.2, 150 mM NaCl		
Temperature	22°C		
Software	BioXTAS RAW version 2.0.2		
Loading concentration (mg/ml)	3.7	5.0	2.0
Loading volume (µl)	425		
Structural Parameters			
Guinier Analysis*			
$I(0)$ (cm^{-1})	0.0231 ± 0.000186	0.0596 ± 0.000169	0.0247 ± 0.000082
R_g (Å)	88.67 ± 1.28	93.17 ± 0.49	54.42 ± 0.30
q range (Å^{-1})	0.005 to 0.0133	0.0047 to 0.0124	0.005 to 0.0227
$q_{min}R_g$ to $q_{max}R_g$	0.444 to 1.178	0.439 to 1.158	0.272 to 1.237
Coefficient of Correlation, R^2	0.981	0.996	0.991
$P(r)$ Analysis (from GNOM**)			
$I(0)$ (cm^{-1})	0.0235 ± 0.000234	0.0595 ± 0.000155	0.0251 ± 0.000085
R_g (Å)	95.97 ± 2.21	95.59 ± 0.40	58.69 ± 0.31
D_{max} (Å)	390	345	213
q range (Å^{-1})	0.0050 to 0.3497	0.0047 to 0.3497	0.0050 to 0.3497
χ^2	0.856	1.050	1.104
Porod Volume estimate (Å^3)	152000	157000	109000
Molecular weight based on volume of correlation (V_c)	80,800	94,600	45,400

* Performed in BioXTAS RAW (Hopkins, J.B. *et al.* (2017) *J Appl Crystallogr* **50**, 1545-1553).
** Svergun, D.I. (1992). *J Appl Crystallogr* **25**, 495-503.

Table S3. Data collection details and analysis statistics for MALS experiments, related to Figure 5.

	mKirrel2 ECD	mKirrel3 ECD Q128A	mKirrel3 ECD WT run 1	mKirrel3 ECD WT run 2	mKirrel3 ECD WT run 3
Experiment Type	SEC-SAXS-MALS				
Instrument	DAWN HELEOS with Optilab T-rEX at BioCAT (APS beamline 18-ID)				
Wavelength	660 nm (for light scattering) and 658 nm (for RI)				
Flow rate	0.6 ml/min				
Chromatography column	Superdex 200 10/300 Increase				
Buffer	10 mM HEPES pH 7.2, 150 mM NaCl				
Refractive index of the solvent (assumed)	1.331				
Temperature	25°C				
Software	ASTRA version 7.3.2.19 (Wyatt)				
Loading volume	425 µl				
Loading concentration (mg/ml)	3.7	2.0	5.0	2.0	0.5
dn/dc*	0.182	0.181	0.181	0.181	0.181
M_n**	97,200 (±6.2%)	54,830 (±7.5%)	111,100 (±6.5%)	105,400 (±4.6%)	97,910 (±5.2%)
M_w†	97,630 (±6.2%)	55,200 (±7.3%)	111,400 (±6.5%)	105,500 (±4.6%)	98,170 (±5.2%)

* dn/dc values are estimated based on predicted N-linked glycosylation content.
** Number-averaged molar mass.
† Weight-averaged molar mass.